

Somatic mutations of cell-free circulating DNA detected by next-generation sequencing reflect the genetic changes in both germinal center B-cell-like and activated B-cell-like diffuse large B-cell lymphomas at the time of diagnosis

Diffuse large B-cell lymphoma (DLBCL) is the most common form of lymphoma, accounting for 30-40% of newly diagnosed cases of non-Hodgkin lymphomas. The molecular heterogeneity of DLBCL has been deciphered by gene expression profiling, and DLBCL have been divided into three main molecular subtypes: the germinal center B-cell-like (GCB) subtype, the activated B-cell-like (ABC) subtype, and the primary mediastinal B-cell lymphoma subtype with distinct clinical outcomes and responses to immunochemotherapy. Next-generation sequencing (NGS) technologies, which allow for massive, parallel, high-throughput DNA sequencing, have emerged over the past decade and have provided new insights into the genomic characterization of DLBCL. Recurrent single nucleotide variants (SNV) are now well defined and provide new therapeutic opportunities for the three molecular subtypes. The SNV target genes play a crucial role in several pathways, including B-cell receptor signaling (*CD79A/CD79B*), NFκ-B (*CARD11*), Toll-like receptor signaling (*MYD88*), immunity (*CD58*, *TNFSRF14*, *B2M*), cell cycle/apoptosis (*TP53*, *BCL2*) and epigenetic regulation (*EZH2*, *CREBBP*, *MLL2*).^{1,2}

Recently, whole exome sequencing in breast cancer has shown that mutations observed in the tumor could also be detected in circulating, cell-free DNA (cfDNA) and could be used to detect genetic changes during treatments and relapse, defining the concept of "liquid biopsy".³ In DLBCL, whereas tumor circulating cells or leukemic phase are not usually detectable, clonotypic sequences have been con-

stantly detected in cfDNA extracted from serum/plasma or peripheral blood mononuclear cells.^{4,8}

In this study we sought to determine, by routinely applicable NGS technology, whether the pattern of acquired SNV observed in tumor DNA could also be detected in cfDNA in DLBCL patients at the time of diagnosis. For this purpose, we analyzed 12 DLBCL cases with available matched tumor DNA and plasma collected at the time of diagnosis. Patients harboring typical GCB/ABC-related mutations targeting *CD79A/B*, *EZH2*, *CARD11* or *MYD88* genes, previously identified by the Sanger method, were selected.⁹ This study was approved by the regional ethical committee (numbered as CPP N°01/006/2014).

The main clinical features of the patients are summarized in Table 1. None of the selected cases harbored detectable circulating lymphoma cells by routine blood smear examination. Of note, no peripheral blood cytometry was performed, in accordance with our center's initial staging procedures for DLBCL patients. Tumor DNA was extracted from frozen lymph node samples by standard methods. cfDNA was extracted from archived EDTA-anticoagulated plasma aliquots (1 mL) stored at -80°C using the QIAamp® Circulating Nucleic Acid Kit (Qiagen) (with the QIAvac 24 Plus vacuum manifold, following the manufacturer's instructions), and concentrations were measured using a fluorometric assay (Qubit® dsDNA HS Assay Kit, Life Technologies). The mean cfDNA concentration in plasma was 1.65 ng/μL (range, 0.46-11.2 ng/μL) (Table 1). The cell-of-origin signature was determined by cDNA-mediated annealing, selection, extension, and ligation technology based on the expression of 19 genes, as previously reported.¹⁰ Among the 12 cases analyzed, five belonged to the ABC subgroup, six to the GCB subgroup and one case was unclassified (Table 1).

Tumor DNA was sequenced using an Ion Torrent Personal Genome Machine (Life Technologies). Ten

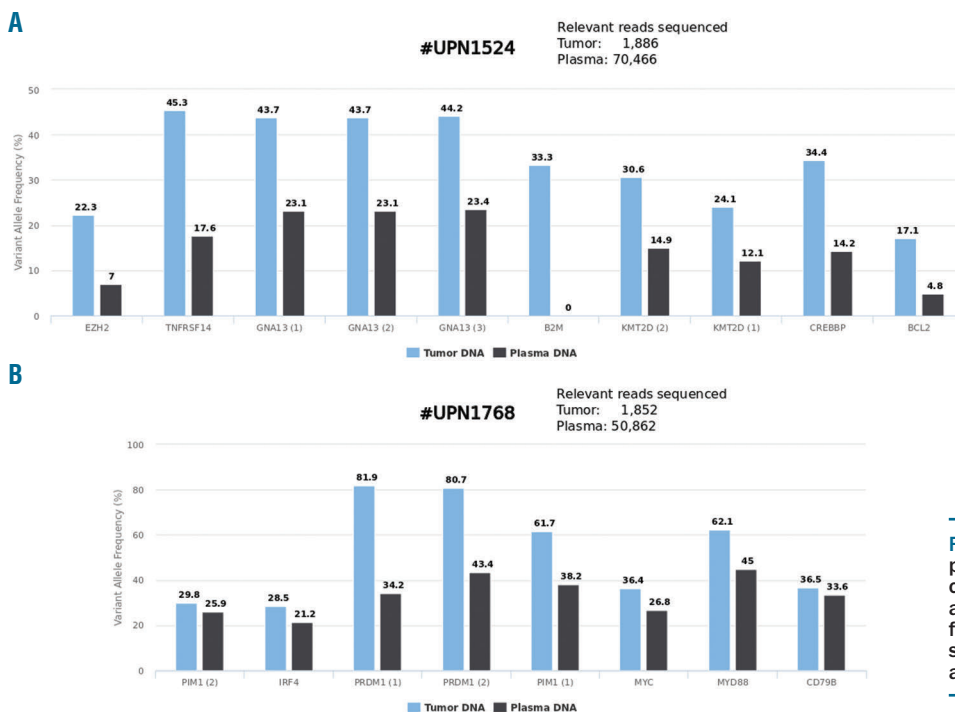


Figure 1. Representative examples of variant allele frequencies observed in tumor DNA and matched circulating cell-free DNA at the time of diagnosis in two different patients (A and B).

Table 1. Clinical characteristics and list of somatic variants (insertion/deletion/ single nucleotide variant) detected by sequencing in tumor DNA and cell-free, plasma circulating DNA. Details of the locations of the mutations are indicated in *Online Supplementary Table S1*.

UPN	Sex	Age (years)	Stage	IPI (score)	LDH (xUNL)	Bone marrow involvement	Phenotype	Gene	Tumor DNA			Circulating DNA			
									VAF (%)	read number	mean VAF (%)	VAF (%)	read number	mean VAF (%)	allele call
964	F	17	IV	3	5	0	GCB	<i>ITPKB (1)</i>	40.9	79/193		2.5	158/6313	Heterozygous	2.02
								<i>ITPKB (2)</i>	40.6	78/192		2.4	152/6260	Heterozygous	
								<i>CARD11</i>	17.1	13/76	40	0.0	0/54	2 Absent	
								<i>EZH2</i>	26.3	76/289		2.8	126/4435	Heterozygous	
								<i>B2M</i>	75.6	102/135		4.0	130/4016	Heterozygous	
1003	F	75	III	3	2.5	0	ABC	<i>ITPKB</i>	35.3	36/102		1.4	22/1540	Heterozygous	1.94
								<i>MYD88</i>	26.5	67/253	40	0.0	0/21	5 Absent	
								<i>CHTA</i>	51.9	14/27		16.7	1/6	Heterozygous	
								<i>CD79B</i>	46.3	93/201		2.1	369/17260	Heterozygous	
1251	M	42	IE	0	0.8	0	GCB	<i>TNFRSF14</i>	52.5	74/141		0.0	0/1113	Absent	0.46
								<i>EZH2</i>	9.8	38/389	31	0.0	0/2519	0 Absent	
								<i>SOC1</i>	30.4	7/23		0.0	0/1053	Absent	
1437	M	76	III	4	5.85	0	ABC	<i>CD79A (1)</i>	17.0	53/318	17	89.1	344/386	89 Heterozygous	11.2
								<i>CD79A (2)</i>	17.0	53/318		89.1	344/386	Heterozygous	
1524	F	45	III	2	1.52	0	GCB	<i>TNFRSF14</i>	45.3	77/170		17.6	539/3064	Heterozygous	1.48
								<i>EZH2</i>	22.3	106/475		7.0	818/11751	Heterozygous	
								<i>KMT2D (1)</i>	24.1	64/266		12.1	1269/10509	Heterozygous	
								<i>KMT2D (2)</i>	30.6	33/108		14.9	1015/6818	Heterozygous	
								<i>B2M</i>	33.3	44/132	34	0.0	0/4555	14 Absent	
								<i>CREBBP</i>	34.4	45/131		14.2	47/331	Heterozygous	
								<i>GNA13 (1)</i>	43.7	52/119		23.1	1909/8254	Heterozygous	
								<i>GNA13 (2)</i>	43.7	52/120		23.1	1920/8314	Heterozygous	
								<i>GNA13 (3)</i>	44.2	53/120		23.4	1946/8312	Heterozygous	
								<i>BCL2</i>	17.1	42/245		4.8	409/8558	Heterozygous	
1528	F	66	III	4	1.39	0	GCB	<i>ITPKB (1)</i>	9.3	14/151		0.0	0/1713	Absent	1.94
								<i>ITPKB (2)</i>	15.2	19/125		0.0	0/3582	Absent	
								<i>ITPKB (3)</i>	15.2	19/125		0.0	0/3577	Absent	
								<i>ITPKB (4)</i>	15.5	19/123		0.0	0/3570	Absent	
								<i>MYD88</i>	37.8	74/196		8.5	161/1888	Heterozygous	
								<i>TNFAIP3</i>	45.7	32/70		5.6	177/3152	Heterozygous	
								<i>EZH2</i>	5.9	44/741		2.1	152/7401	Heterozygous	
								<i>KMT2D</i>	36.1	122/338		5.7	207/3620	Heterozygous	
								<i>B2M</i>	50.0	63/126	31	3.2	78/2465	3 Heterozygous	
								<i>CHTA (1)</i>	39.0	30/77		0.0	0/2130	Absent	
								<i>CHTA (2)</i>	7.7	14/183		0.0	0/9150	Absent	
								<i>CHTA (3)</i>	7.6	14/184		0.0	0/9162	Absent	
								<i>GNA13 (1)</i>	71.0	105/148		0.0	0/2695	Absent	
								<i>GNA13 (2)</i>	71.0	105/148		3.1	82/2672	Heterozygous	
								<i>BCL2(1)</i>	34.1	47/138		4.3	214/4929	Heterozygous	
								<i>BCL2 (2)</i>	32.9	45/137		4.2	209/5013	Heterozygous	
								<i>MEF2B</i>	33.3	137/411		5.9	654/11153	Heterozygous	
1559	F	83	IE	1	0.8	0	ABC	<i>CD58</i>	92.9	92/99		0.0	0/13231	Absent	0.618
								<i>MYD88</i>	51.8	187/361		0.0	0/11427	Absent	
								<i>CREBBP</i>	46.3	154/333	64	0.0	0/5663	<1 Absent	
								<i>TP53</i>	89.0	105/118		0.0	0/13012	Absent	
								<i>CD79A (1)</i>	52.0	122/235		0.5	20/3930	Absent	
								<i>CD79A (2)</i>	52.0	122/235		0.5	20/3932	Absent	
1586	F	62	III	2	0.85	0	NA	<i>TNFRSF14</i>	13.8	44/318		2.1	6/284	Heterozygous	1.31
								<i>EZH2</i>	13.8	41/298		0.0	0/6575	Absent	
								<i>STAT6</i>	18.9	83/439	20	0.0	2/5517	<1 Absent	
								<i>CREBBP</i>	33.6	49/146		1.3	65/4894	Absent	
								<i>GNA13</i>	17.7	11/62		0.0	0/4391	Absent	
1623	M	53	IV	2	1.03	0	GCB	<i>TNFRSF14</i>	34.8	146/419		19.3	694/3587	Heterozygous	0.95
								<i>EZH2</i>	9.9	57/575		1.8	62/3480	Heterozygous	
								<i>STAT6</i>	15.4	79/514		5.1	200/3889	Heterozygous	
								<i>CREBBP (1)</i>	23.2	166/717	18	11.6	489/4222	11 Heterozygous	
							<i>CREBBP (2)</i>	14.0	54/387		10.1	328/3239	Heterozygous		
							<i>CD79B</i>	17.1	83/486		18.0	839/4651	Heterozygous		
							<i>MEF2B</i>	11.8	74/626		9.9	1283/12969	Heterozygous		

Table 1 (continued on the next page).

(continued from the previous page).

UPN	Sex	Age (years)	Stage	IPI (score)	LDH (xUNL)	Bone marrow involvement	Phenotype	Gene	Tumor DNA			Circulating DNA			
									VAF (%)	read number	mean VAF (%)	VAF (%)	read number	mean VAF (%)	allele call
1631	M	64	I	2	1.54	0	ABC	<i>MYD88</i>	49.8	220/442		11.7	655/5586	Heterozygous	1.1
								<i>PIM1</i>	20.6	14/68		2.7	130/4797	Heterozygous	
								<i>CARD11 (1)</i>	47.1	99/210		5.1	154/3028	Heterozygous	
								<i>CARD11 (2)</i>	47.9	68/142	35	5.5	344/6300	5 Heterozygous	
								<i>STAT6</i>	18.1	96/532		4.3	570/13250	Heterozygous	
								<i>TP53</i>	32.4	72/222		3.9	522/13317	Heterozygous	
								<i>CD79B</i>	26.7	52/195		3.3	386/11853	Heterozygous	
								<i>TNFRSF14</i>	75.8	47/62		82.3	2400/2915	Heterozygous	
								<i>MYD88</i>	27.5	133/483		7.1	1616/22541	Heterozygous	
								<i>EZH2</i>	24.0	126/526		32.8	3259/9939	Heterozygous	
1639	M	69	IV	2	2.4	0	GCB	<i>KMT2D (1)</i>	33.8	187/554		35.0	5878/16784	Heterozygous	10.2
								<i>KMT2D (2)</i>	28.3	13/46	39	22.9	671/2929	34 Heterozygous	
								<i>CREBBP</i>	37.0	17/46		30.6	2918/9530	Heterozygous	
								<i>BCL2 (1)</i>	45.8	11/24		31.5	223/709	Heterozygous	
								<i>BCL2 (2)</i>	53.0	98/185		28.2	2267/8032	Heterozygous	
								<i>EP300</i>	29.6	34/115		38.3	4597/11990	Heterozygous	
								<i>MYD88</i>	62.1	216/348		45.0	5936/13194	Heterozygous	
								<i>IRF4</i>	28.5	75/263		21.2	929/4374	Heterozygous	
								<i>PIM1 (1)</i>	61.7	145/235		38.2	1541/4030	Heterozygous	
								<i>PIM1 (2)</i>	29.8	34/114	52	25.9	987/3812	34 Heterozygous	
1768	M	83	IV	3	4.2	0	ABC	<i>PRDM1(1)</i>	81.9	149/182		34.2	1273/3724	Heterozygous	1.82
								<i>PRDM1(2)</i>	80.7	221/274		43.4	5076/11689	Heterozygous	
								<i>MYC</i>	36.4	102/280		26.8	262/979	Heterozygous	
								<i>CD79B</i>	36.5	57/156		33.6	3041/9060	Heterozygous	

ABC: activated B-cell-like; GCB: germinal center B-cell-like; In/del: insertion/deletion; LDH: lactate dehydrogenase; IPI: International Prognosis Index; SNV: single nucleotide variant; UPN: unique personal number; UNL: upper limit of normal value; VAF: variant allele frequency.

nanograms of genomic DNA were submitted to NGS using a laboratory-developed Lymphopanel set, designed to identify mutations in 34 genes relevant to lymphomagenesis (*Online Supplementary File S1A*). This design covers 87,703 bases and generates 872 amplicons. Amplified libraries (Ion AmpliSeq™ Library Kit 2.0) were submitted to emulsion polymerase chain reaction with the Ion OneTouch™ 200 Template Kit (Life Technologies) using the Ion OneTouch™ System (Life Technologies) according to the manufacturer's instructions. The templated Ion Sphere™ Particles were enriched with the Ion OneTouch™ Enrichment System and loaded and sequenced on an Ion 316™ v2 Chip (Life Technologies).

After alignment to a reference genome sequence (hg19) and a variant calling procedure, variants were filtered through a dedicated bioinformatic pipeline that eliminated synonymous variants and variants with a variant allele frequency (VAF) greater than 1% in the 1000 genome database (considered as polymorphisms). Only non-synonymous SNV/In/Del with a quality score >22 and/or confirmed by a Sanger experiment were retained as acquired somatic mutations in lymphoma cases and were used for the subsequent sequencing of the matched cfDNA (for the detailed pipeline see *Online Supplementary File S1B*). Somatic mutations identified in tumor DNA were used to build a hot-spot file enabling higher sensitivity tracking of somatic mutations in circulating DNA.

In order to increase the sensitivity and specificity of variant detection in cfDNA, we exclusively amplified amplicons targeting mutations detected in the corresponding tumor DNA by the complete Lymphopanel by performing a dedicated sequencing procedure with a pool of oligonucleotide primers selected among the 872 pairs provided by

Life Technologies. The procedure to make libraries and sequence amplicons was the same as that for tumor DNA but used a 314™ v2 Chip. When possible, circulating DNA was extracted and sequenced from two different aliquots of plasma.

The SNV/In/Del detected in both tumor and circulating DNA are indicated in Table 1 with their corresponding VAF. As expected, we identified a typical SNV pattern in the five ABC DLBCL cases, including mutations targeting *MYD88*, *CD79A/B*, *PIM1*, *PRDM1*, *CARD11* or *IRF4*, whereas *EZH2*, *BCL2*, *GNA13*, or *TNFRSF14* were mutated in the unclassified and GCB DLBCL cases. *MLL2 (KMT2D)*, *CREBBP* or *ITPKB* were targeted by somatic mutations shared in the two cell-of-origin subtypes. The sequencing depths obtained for each sample and targets are indicated in Table 1.

The mean number of reads targeting the mutated regions for tumor DNA was 241 (range, 23-741) as compared to 5,987 (range, 6-22,541) for plasma DNA, indicating a 24-fold mean depth sequencing increase. The mean VAF in the tumor DNA was 35% (range, 17-64%) as compared to a mean of 11% for plasma DNA (range, 2-89%) (Table 1).

In 11/12 DLBCL cases, we observed somatic mutations in cfDNA, similar or partially similar to those observed in the tumor (Figure 1, Table 1 and *Online Supplementary Figure S1*). We defined the concordance rate as the ratio of the number of mutated cfDNA genes and the number of mutated tumor DNA genes. This rate ranged from 33% to 100% (5 cases) in the 11/12 cases with detected mutated cfDNA. Overall, the median concordance rate between tumor DNA and cfDNA was 85%.

In one case (#1251), SNV observed in the tumor DNA were not detected in plasma DNA. In another case (#1559),

SNV were barely detectable (VAF of 0.5% for two variants). Of note, both cases displayed limited disease (stage I or II) and normal lactate dehydrogenase levels, indicating that the amount of tumor-specific circulating cfDNA is at least partially related to tumor burden. Despite a low amount of circulating DNA extracted from plasma for cases #1251 and #1559, we obtained adequate sequencing quality and depth (the overall number of reads sequenced with mutated targets was 4,685 and 51,195 respectively; Table 1), indicating that in some rare cases, tumor-specific cfDNA is absent or beneath the level of sensitivity of the NGS method used. Of note, in case #1631 characterized by limited stage I disease, SNV were detected with a mean VAF of 5.2% in plasma DNA, as compared to a mean VAF of 34.6% in the tumor DNA (Table 1). In contrast, cases #1639 and #1768 (both with stage IV disease and elevated levels of lactate dehydrogenase) displayed a high proportion of tumor-specific circulating DNA, as indicated by the high VAF observed (Table 1). Interestingly, in these two cases, the sub-clonal distribution of certain mutations, as indicated by the VAF distribution of each individual variant, was also observed in cfDNA, suggesting that sequencing cfDNA can reflect the SNV pattern observed in tumor cells in some instances (Figure 1 and *Online Supplementary Figure S1*). In case #1524, despite a sufficient number of relevant reads (> 4,000) we failed to detect the *B2M* SNV present in the lymph node biopsy. This result was confirmed by manual Integrative Genomics Viewer checking, suggesting that the *B2M* SNV is present only in a subclone caught in the biopsy sample but not highlighted by the cfDNA that reflects the entire tumor burden.

By contrast, in some cases, the number of target reads was clearly insufficient for adequate SNV detection (case #964, *CARD11*; case #1003, *MYD88*; Table 1), most likely reflecting the low amount of cfDNA available rather than a true clonal divergence between tumor DNA and cfDNA. This was not observed in cases with higher amounts of cfDNA.

Failure to detect SNV in cfDNA appears related more to the proportion of tumor-specific DNA than to the total amount or quality of total cfDNA. Of note, we failed to find any tumor-related SNV in DNA extracted from 11/12 samples of peripheral blood mononuclear cells using this approach (*data not shown*), indicating that serum or plasma is preferable for the detection of mutated circulating DNA. In a large cohort of cases of Hodgkin lymphoma, mantle cell lymphoma and DLBCL, increased levels of plasma DNA (determined using quantitative polymerase chain reaction for the β -globin gene) were associated with advanced stage disease, presence of B-symptoms, elevated lactate dehydrogenase levels, and age >60 years also indicating that the amount of circulating DNA is partially related to tumor burden.⁸ Furthermore, it was shown in a cohort of patients with Epstein-Barr virus-positive lymphoma that serum and plasma were equivalent for detecting lymphoma-specific DNA but that only the lymphoma-specific DNA could be used to monitor disease response in lymphoma.⁷

To our knowledge this is the first report of the detection of non-immunoglobulin somatic mutations in DLBCL from circulating DNA by routine NGS, enabling the identification of lymphoma-specific cfDNA. Other quantitative approaches, including digital polymerase chain reaction, are also suitable and could be used in this setting for detecting recurrent translocations or mutations.¹¹ More recently LymphoSIGHT[®], a high-throughput DNA sequencing method, was developed to detect and quantify circulating tumor DNA as minimal residual disease and was able to predict both early treatment failure and relapse in patients

with newly diagnosed DLBCL, chronic lymphocytic leukemia or acute lymphoblastic leukemia.¹²⁻¹⁵ This approach is based on tumor DNA amplification using locus-specific primer sets for the immunoglobulin heavy/light-chain which failed in a substantial number of cases of DLBCL. Importantly the Lymphopanel used in this study is able to detect at least one acquired SNV in 95% of DLBCL cases at initial diagnosis (*manuscript in preparation*) and may, therefore, constitute a simple, routinely applicable test to provide the cell-of-origin subtype or to detect targetable mutations at the time of diagnosis or relapse. However, its capacity to detect minimal residual disease with a high level of sensitivity remains to be determined and we can hypothesize that at least 5-10% of DLBCL cases will not display any SNV detectable by our Lymphopanel. Furthermore, cfDNA sequencing was successfully performed using the entire Lymphopanel (including the 34 targeted genes) in one case (*data not shown*), indicating that this approach is feasible without the knowledge of the tumor variant calling. However this requires an increase in the sequencing depth capacity and entails a substantial increase of costs.

To conclude, our results indicate that cfDNA can also be used in DLBCL to detect somatic variants, validating the concept of "liquid biopsy" in this type of tumor.³ These preliminary results have prompted us to start a prospective study with the aim of serially sequencing cfDNA during DLBCL treatment and follow-up (registered at *clinicaltrials.gov* as NCT02339805). If these preliminary results are confirmed by a prospective study, new strategies should be proposed for both diagnosis and treatment tailoring based on the simple detection and quantification of SNV in plasma.

Elodie Bohers,¹ Pierre Julien Viailly,¹ Sydney Dubois,¹ Philippe Bertrand,¹ Catherine Maingonnat,¹ Sylvain Mareschal,¹ Philippe Ruminy,¹ Jean-Michel Picquenot,² Christian Bastard,¹ Fabienne Desmots,³ Thierry Fest,³ Karen Leroy,⁴ Hervé Tilly,^{1,5} and Fabrice Jardin^{1,5}

¹INSERM U918, Centre Henri Becquerel, Université de Rouen, IRIB; ²Department of Pathology, Centre Henri Becquerel, Rouen; ³UMR INSERM U917, CHU Pontchaillou, Rennes; ⁴INSERM U955, Henri Mondor Hospital, Creteil; and ⁵Department of Clinical Hematology, Centre Henri Becquerel, Rouen, France

Correspondence: fabrice.jardin@chb.unicancer.fr
doi:10.3324/haematol.2015.123612

Key words: diffuse large B-cell lymphoma, NGS, liquid biopsy, mutations.

Information on authorship, contributions, and financial & other disclosures was provided by the authors and is available with the online version of this article at www.haematologica.org.

References

- Morin RD, Gascoyne RD. Newly identified mechanisms in B-cell non-Hodgkin lymphomas uncovered by next-generation sequencing. *Semin Hematol.* 2013;50(4):303-313.
- Roschewski M, Staudt LM, Wilson WH. Diffuse large B-cell lymphoma-treatment approaches in the molecular era. *Nat Rev Clin Oncol.* 2014;11(1):12-23.
- Diaz LA, Jr., Bardelli A. Liquid biopsies: genotyping circulating tumor DNA. *J Clin Oncol.* 2014;32(6):579-586.
- He J, Wu J, Jiao Y, et al. IgH gene rearrangements as plasma biomarkers in Non-Hodgkin's lymphoma patients. *Oncotarget.* 2011; 2(3):178-185.
- Hosny G, Farahat N, Hainaut P. TP53 mutations in circulating free DNA from Egyptian patients with non-Hodgkin's lymphoma. *Cancer Lett.* 2009;275(2):234-239.

6. Mussolin L, Burnelli R, Pillon M, et al. Plasma cell-free DNA in paediatric lymphomas. *J Cancer*. 2013;4(4):323-329.
7. Jones K, Nourse JP, Keane C, et al. Tumor-specific but not nonspecific cell-free circulating DNA can be used to monitor disease response in lymphoma. *Am J Hematol*. 2012;87(3):258-265.
8. Hohaus S, Giachelia M, Massini G, et al. Cell-free circulating DNA in Hodgkin's and non-Hodgkin's lymphomas. *Ann Oncol*. 2009;20(8):1408-1413.
9. Bohers E, Mareschal S, Bouzelfen A, et al. Targetable activating mutations are very frequent in GCB and ABC diffuse large B-cell lymphoma. *Genes Chromosomes Cancer*. 2014;53(2):144-153.
10. Lanic H, Mareschal S, Mechken F, et al. Interim positron emission tomography scan associated with international prognostic index and germinal center B cell-like signature as prognostic index in diffuse large B-cell lymphoma. *Leuk Lymphoma*. 2012;53(1):34-42.
11. Shuga J, Zeng Y, Novak R, et al. Single molecule quantitation and sequencing of rare translocations using microfluidic nested digital PCR. *Nucleic Acids Res*. 2013;41(16):e159.
12. Armand P, Oki Y, Neuberger DS, et al. Detection of circulating tumour DNA in patients with aggressive B-cell non-Hodgkin lymphoma. *Br J Haematol*. 2013;163(1):123-126.
13. Logan AC, Vashi N, Faham M, et al. Immunoglobulin and T cell receptor gene high-throughput sequencing quantifies minimal residual disease in acute lymphoblastic leukemia and predicts post-transplantation relapse and survival. *Biol Blood Marrow Transplant*. 2014;20(9):1307-1313.
14. Logan AC, Zhang B, Narasimhan B, et al. Minimal residual disease quantification using consensus primers and high-throughput IGH sequencing predicts post-transplant relapse in chronic lymphocytic leukemia. *Leukemia*. 2013;27(8):1659-1665.
15. Roschewski M, Dunleavy K, Pittaluga S, et al. Monitoring of circulating tumor DNA as minimal residual disease in diffuse large B-cell lymphoma. *Blood*. 2014;124(21):139 Abstr.